Vol 453|1 May 2008|doi:10.1038/nature06886

LETTERS

The sculpting of Jupiter's gossamer rings by its shadow

Douglas P. Hamilton[1] & Harald Krüger[2,3]

Dust near Jupiter is produced when interplanetary impactors collide energetically with small inner moons, and is organized into a main ring, an inner halo, and two fainter and more distant gossamer rings[1,2]. Most of these structures are constrained by the orbits of the moons[3] Adrastea, Metis, Amalthea and Thebe, but a faint outward protrusion called the Thebe extension behaves differently and has eluded understanding. Here we report on dust impacts detected during the Galileo spacecraft's traversal of the outer ring region[4]: we find a gap in the rings interior to Thebe's orbit[5], grains on highly inclined paths, and a strong excess of submicrometre-sized dust just inside Amalthea's orbit. We present detailed modelling that shows that the passage of ring particles through Jupiter's shadow creates the Thebe extension and fully accounts for these Galileo results. Dust grains alternately charge and discharge when traversing shadow boundaries, allowing the planet's powerful magnetic field to excite orbital eccentricities[6] and, when conditions are right, inclinations as well.

Jupiter's dusty rings were discovered by the Voyager spacecraft in 1979 and have subsequently been investigated with Earth- and space-based telescopes[5,7] as well as *in situ* spacecraft[1,3,8,9]. These observations have revealed a broad but very tenuous distribution of dust straddling the orbits of four small inner moons. For the most part, these moonlets bound the radial and vertical extent of the various ring structures, as summarized in Fig. 1a. There is, however, one major discrepancy: the Thebe extension, which has a vertical profile that matches Thebe's orbital excursions, but lies fully outside its source moonlet. Some dynamical process not considered by the standard ring models is clearly at work, but why does it single out the Thebe extension?

A unique source of data on the outer jovian rings was provided by Galileo, which passed through the tenuous Thebe and Amalthea rings in 2002 and 2003 (Fig. 1b). The spacecraft's impact-ionization dust detector[10] recorded ~100 impacts of micrometre- and submicrometre-sized dust grains, providing *in situ* information on particle sizes, speeds, impact directions and impact rates. Although the initial analysis of these data appeared in refs 4 and 11, it has not yet been reported in a scientific journal. The dust detector found a sharp transition between the Amalthea and Thebe rings in agreement with imaging, but other results were less expected. For example, some dust grains follow orbits tilted by ~20° from Jupiter's equator, which is surprising because particles in the visible rings have orbits tilted by only ~1°. The instrument also measured a reduction of particle flux interior to Thebe's orbit that was unanticipated because of the seemingly smooth increase of brightness of the optical image (red region of Fig. 1a; note that the vertical blue stripe is probably an artifact); see also ref. 5. Finally, the smallest detected dust grains, with radii of 0.2–0.3 μm, are far less prevalent near Thebe than near Amalthea, a difference that highlights the importance of electromagnetic forces[12]. These three results, detailed in Fig. 2a–c, nicely complement images of the Thebe extension. The combined constraints allow us to demonstrate convincingly that electromagnetic processes involving Jupiter's shadow[6] govern the planet's gossamer rings.

The orbits of micrometre-sized ring particles are dominated by Jupiter's gravity, but are also subject to electromagnetic forces and, to a far lesser extent, radiation pressure from the Sun. Dust grains acquire electric charges in Jupiter's vicinity by sweeping up local plasma and by photoemission[6,13] in which sunlight incident on a dust grain liberates electrons. Typically the charge is driven rapidly to an equilibrium value that depends on the dust-grain speed, the plasma composition and temperature, and the strength of solar radiation. These effects balance at one value in Jupiter's shadow and at another, larger, value in full sunlight.

Without planetary shadowing, the effects of electromagnetic forces on the sizes (semimajor axes a) and shapes (eccentricities e) of ring

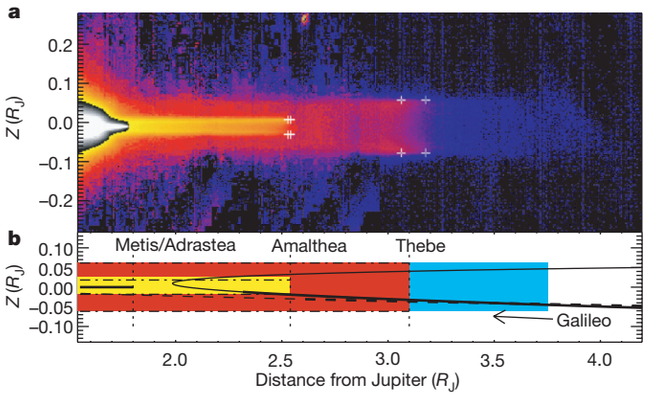

Figure 1 | Overview of Jupiter's diffuse ring system. a, Jupiter's gossamer rings as seen by Galileo from a location near the planet's equatorial plane (false colour: adapted from ref. 1). Galileo observations[1,3] first showed that the ring system has at least four distinct components: (1) the main ring (in white) projecting inward from the two moonlets Metis and Adrastea, (2) the vertically extended halo (white) with thickness $0.1R_J$ (R_J = 71,492 km) interior to the main ring, (3) a gossamer ring associated with the satellite Amalthea (small yellow rectangle), and (4) an even fainter ring associated with Thebe (large red rectangle). Crosses mark the extremes of the radial and vertical motions of the two moons caused by their eccentric and inclined orbits. The thicknesses of the two outer rings exactly match the vertical excursions of the two source satellites, and ring material appears to extend primarily inward from all four moonlets[1,3]. The Thebe extension is the faint material (in blue) located outside Thebe's orbit. **b**, Galileo's trajectories during the ring passages on 5 November 2002 (solid line) and 21 September 2003 (dashed line). Dust data were acquired from most of the inbound legs (thick lines), but a spacecraft anomaly prevented measurements inside $2.33R_J$ and during the outbound leg. We colour-code the ring components, and indicate the approximate locations of the moons' orbits by vertical dashed lines.

[1]Astronomy Department, University of Maryland, College Park, Maryland 20742-2421, USA. [2]Max-Planck-Institut für Sonnensystemforschung, Max-Planck-Strasse 2, 37191 Katlenburg-Lindau, Germany. [3]Max-Planck-Institut für Kernphysik, Postfach 103980, 69029 Heidelberg, Germany.

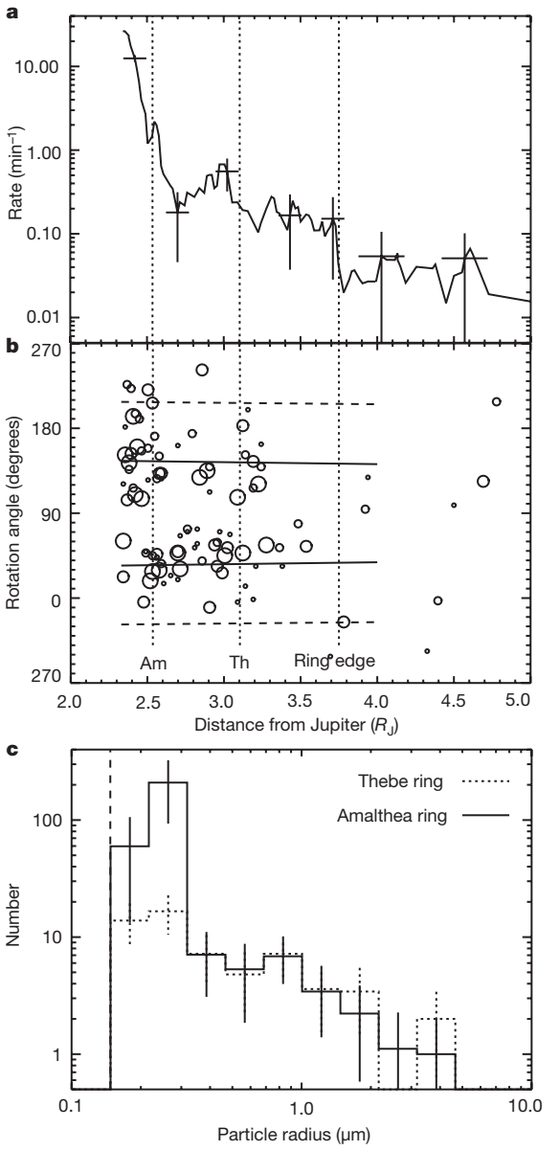

Figure 2 | Galileo dust data. a, Impact rate of submicrometre-sized dust particles onto the Galileo dust detector[10] during the 5 November 2002 ring passage. The rate increased by a factor of 1,000 as the spacecraft moved inward from $3.75R_J$ (right to left). The main rise at Amalthea's orbit (inner edge of the plot) is also seen in all other instrument channels, and corresponds to the transition from the Thebe to the Amalthea ring (Fig. 1). The next-most-significant feature is the dip in the rate by a factor of ~3 from $3.0R_J$ to $2.7R_J$. Although the error bars (±1s.d.) are large, we believe that the feature is real, as it also appears in similar data for larger particles and in Galileo's second ring passage. Furthermore, the dip is also consistent with a detailed analysis of the Galileo images[5]. As indicated by the error bars, much of the fine structure at significantly lower impact rates is probably due to small number statistics. **b**, Distribution of dust grain trajectories. Larger symbols indicate larger particles. The rotation angle indicates the phase of the spinning spacecraft; the detector points closest to ecliptic north (south) at rotation angle 0° (180°). An analysis of the 140° field of view of the instrument combined with the 60° angle between the sensor and spin axes[4,10,11] and the spacecraft trajectory and spin axis pointing shows that particles on circular uninclined orbits could strike the detector when the spacecraft had a rotation angle between 30° and 150°. We indicate this detection limit with a pair of solid lines, and another for orbits with 20° tilts with dashed lines. A significant number of both large and small impacts occur outside the solid lines, indicating that some ring particles have large inclinations of ~20°. **c**, Radii of detected dust grains in the Thebe ring (2.54–3.10 R_J; dotted) and the Amalthea ring (2.33–2.54 R_J; solid). Error bars, ±1s.d. The distributions are similar, except for a very strong excess of 0.2 μm grains in the Amalthea ring.

particle orbits average to zero over satellite orbital periods (~12 h) (ref. 14). With shadowing, however, significant changes to semi-major axes and eccentricities can accumulate in phase over the ~6 month timescale during which the long axes of elliptical orbits slowly rotate (or precess) in space. This effect is known as a shadow resonance[6], and it produces a ring that is asymmetric and offset away from the Sun (Fig. 3c), similar to rings driven by radiation pressure[15].

As the shadow resonance is a fully electromagnetic effect and magnetic fields do no work, energy measured in the reference frame that co-rotates with Jupiter's field is conserved. This constraint leads

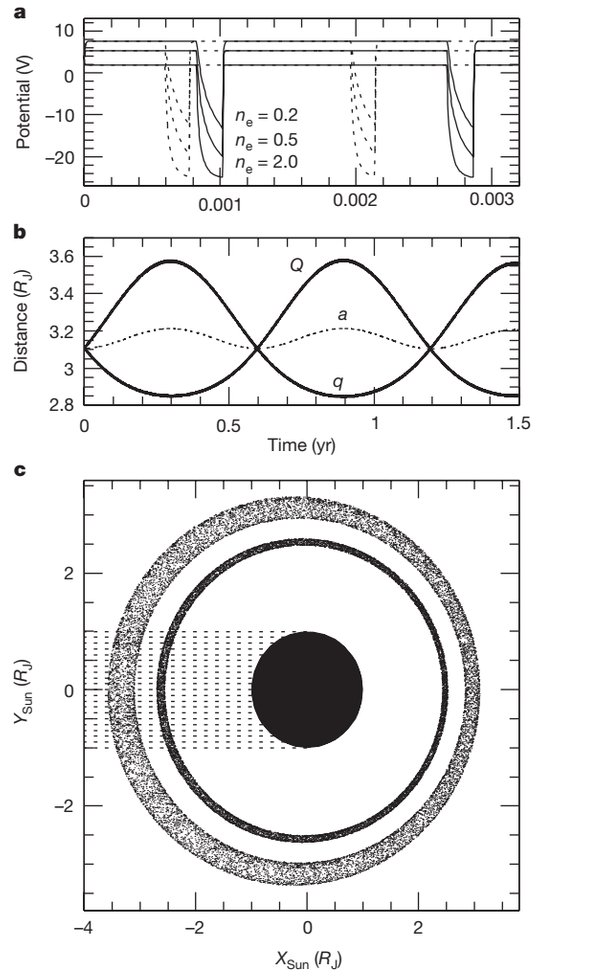

Figure 3 | Variations of the electric potential during shadow passages. a, Electric potential for 3.2 μm dust grains from Amalthea (dotted lines) and Thebe (solid lines) as a function of time. We show charge histories for three different assumed plasma densities n_e in a simple two-component plasma model as dust grains travel from sunlight (flat curves) into Jupiter's shadow (dips to lower potentials) and out again. Dust in a plasma tends to charge negatively, and higher plasma densities lead to lower grain potentials, both in sunlight and in shadow. Sunlight raises equilibrium potentials because the photoelectric effect ejects electrons from a dust grain's surface. In reality, plasma properties probably vary with distance both from Jupiter and the equatorial plane, but we find that these non-uniform distributions lead to changes in orbital behaviour only over timescales much longer than those considered here, validating our simplifying assumption (compare ref. 19). **b**, The orbital evolution of a 3.2 μm dust grain launched from Thebe into an $n_e = 2.0\ \mathrm{cm}^{-3}$ plasma; we plot the grain's pericentre distance $q = a(1 - e)$, semimajor axis a, and apocentre distance $Q = a(1 + e)$. Orbital evolution is due to the shadow resonance discussed in the text; note that dust spreads more easily outward from Thebe (at $3.1R_J$) than inward. **c**, A numerical simulation of the asymmetric Amalthea and Thebe rings formed by 3.2 μm dust grains moving in an $n_e = 2.0\ \mathrm{cm}^{-3}$ plasma and crossing through the planet's shadow (stippled region).

to a constant of the motion (the dimensionless Jacobi constant):

$$C_J = \frac{R_{syn}}{a} + 2\sqrt{\frac{a(1-e^2)}{R_{syn}}}\cos i$$

where i is a ring particle's orbital inclination and $R_{syn} \approx 2.25R_J$ (here R_J is Jupiter's radius) is the radius of the synchronous orbit where a ring particle circles Jupiter at the same rate that the planet rotates[6].

Particles blasted off satellites start on nearly circular orbits around Jupiter, because satellite orbital speeds ($\sim$25 km s^{-1}) completely dominate the small ejection speeds ($\sim$50 m s^{-1}). In the Thebe ring, $a > R_{syn}$ and dynamical evolution leads to $e \gg i$, as the dominant $\mathbf{v} \times \mathbf{B}$ forces are primarily radial (here $\mathbf{v}$ is the velocity of the dust grain relative to Jupiter's magnetic field, $\mathbf{B}$). Thus the equation shows that the semimajor axis and eccentricity increase in tandem, causing dust to spread more easily outward from Thebe than inward, as indicated by Fig. 3b. In fact, dust launched on a circular orbit from Thebe at $a/R_{syn} = 1.38$ has $C_J = 3.074$; by simultaneously taking $a \to \infty$ and $e = 1$, we find that the smallest possible pericentre distance is $q = a(1-e) = 2.66R_J$, about $0.4R_J$ inside Thebe's orbit at $3.1R_J$, while the most distant orbit point $Q = a(1+e)$ can grow without bound. Thus, perturbations from an arbitrary time-varying dust grain charge can bring the dust grain at most $0.4R_J$ inward from Thebe or about halfway to synchronous orbit. This hard limit on the inner extent of the Thebe dust ring provides a natural explanation for the existence of the gap in the dust number density measurements visible at $\sim 2.7R_J$ in Fig. 2a.

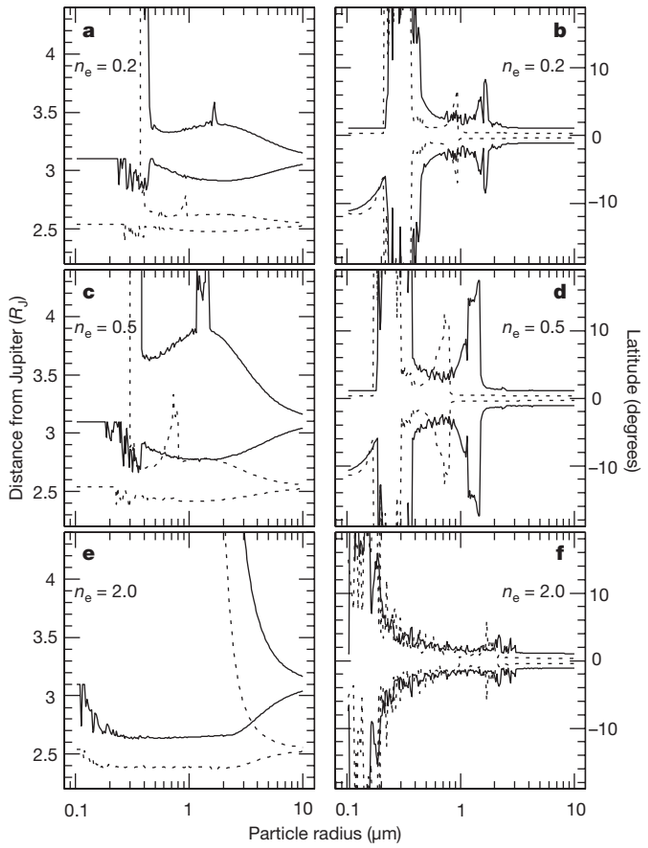

Figure 4 | Radial and vertical mobility of dust. Here we plot numerically determined minimum and maximum distances (left plots) and latitudes (right plots) reached by different-sized ring particles within two years of launch from Thebe (solid curves) and Amalthea (dotted curves). Three different charging histories parameterized by n_e and 600 separate numerical simulations are presented here. The mobility of dust grains is enhanced by two factors: (1) small particle sizes which have larger electromagnetic perturbations, and (2) slow pericentre precession rates which allow the shadow resonance to pump eccentricities to extremely high values[6]. The total precession rate is the sum of a constant gravitational term and an electromagnetic contribution that is dependent on particle size and electric charge[14]. The two terms have the same sign for low plasma densities and are comparable in strength for particle radii of $\sim$2 μm (near the peaks in the radial plots). For larger particles, electromagnetic perturbations weaken and radial mobility decreases. Smaller particles precess so rapidly (owing to electromagnetic perturbations) that changes to eccentricity can add together in phase for only short periods of time and again mobility decreases. **a**, **b**, For $n_e = 0.2$ cm^{-3}, dust grains larger than $\sim$0.5 μm cannot reach outward to the distance observed in Fig. 1 ($3.75R_J$) nor can they attain latitudes in excess of 10°. **c**, **d**, With a plasma density of 0.5 cm^{-3}, micrometre-sized dust from Thebe can extend out to $\sim 4R_J$ and attain latitudes of nearly 20°, as required by the observations. **e**, **f**, For $n_e = 2.0$ cm^{-3}, micrometre-sized dust grains cannot reach large latitudes and dust grains smaller than 2–3 μm escape from the ring entirely. An extremely slow pericentre precession rate, caused by nearly equal and opposite gravitational and electromagnetic terms, allows the shadow resonance to facilitate escape.

We ran a number of dynamical simulations including gravitational, electromagnetic and radiation forces[14] to test our analytic prediction of a gap in the ring particle number density. A critical parameter in these simulations is the plasma density, which has not been measured. Accordingly, we ran the model for a number of different plasma densities (n_e) and display three of them ($n_e = 0.7$, 0.5 and 2.0 cm^{-3}) in Fig. 4. All of the numerical simulations support the existence of an inner boundary, despite the fact that radiation pressure prevents the energy integral from being strictly obeyed. Over much longer timescales, diffusion induced by radiation pressure or dissipative Poynting-Robertson drag can cause material to leak inward from Thebe. Alternatively, ring material detected inside $2.7R_J$ may simply have originated from Amalthea, as suggested by Fig. 4c.

We now compare this suite of models to the other observations discussed above. The visual appearance of the Thebe extension in Fig. 1a requires grains with radii larger than $\sim$2 μm (ref. 5), significant radial extensions, and low orbital inclinations. The latitude plots of Fig. 4 indicate that particles of the right size do maintain low inclinations for all three plasma densities, but for the most tenuous $n_e = 0.2$ cm^{-3} plasma no micrometre-sized material should reach the outer edge of the Thebe extension at $3.75R_J$. Requiring that the shadow resonance be strong enough to push material out to $3.75R_J$ therefore puts a lower limit on the plasma number density, which in our simple model is $n_e > 0.5$ cm^{-3}. Only the models shown in Fig. 4c–f are viable.

There are several reasons why the Amalthea ring does not show a similar extension[5]. First, the electromagnetic force (and hence the shadow resonance) is significantly weaker at Amalthea than at Thebe (note the less perturbed Amalthea ring in Fig. 3c), and in fact vanishes just $\sim 0.3R_J$ inward at synchronous orbit where a ring particle's velocity relative to the magnetic field is zero. In addition, dust grains on crossing orbits survive against recollision with satellites for only $\sim$100 yr near Amalthea, but 25 times longer near Thebe owing to that satellite's smaller size, larger orbital inclination, and greater distance from Jupiter. Finally, an Amalthea extension less than a few per cent of the brightness of the Amalthea ring would be masked by the background debris from Thebe.

Galileo's dust detector observed a significant population of particles with orbits tilted by $\gtrsim 20°$. The models indicate that for certain plasma conditions, particle orbits do in fact attain large inclinations (Fig. 4b, d, f). The mechanism forcing the larger grains to high latitudes is a vertical shadow resonance, in which the line of nodes (the intersection of the orbit plane with Jupiter's equatorial plane) rotates extremely slowly, allowing inclinations to be pumped systematically. Similar to the standard shadow resonance, this requires a near cancellation between gravitational and electromagnetic perturbations to the nodal precession rate, which occurs for dust grains with a specific charge-to-mass ratio. Outside synchronous orbit, positive orbit-averaged charges[14] and therefore low plasma densities are needed.

The vertical shadow resonance forces micrometre and submicrometre grains onto orbits inclined by up to 20°, nicely matching the observed dust trajectories (Fig. 2b). Positive orbit-averaged charges indicate a plasma density $n_e < 2.0\,cm^{-3}$ in our simple model. Only the models shown in Fig. 4c, d satisfy both this and the previous constraint.

Finally, Galileo observed a strong excess of 0.2–0.3 μm dust grains at Amalthea (Fig. 2c). Figure 4 shows that, for all modelled plasma densities, electromagnetic forces cause positively-charged particles smaller than ~0.3 μm to escape entirely from the ring region[12,16]. For our favoured plasma density of $n_e = 0.5\,cm^{-3}$ (Fig. 4c, d), the distance plot shows that a narrow size range from 0.2 to 0.3 μm is retained in the Amalthea ring but escapes from the Thebe ring. This occurs because the shadow resonance, like all electromagnetic effects on ring particles, is weaker near the synchronous orbit just interior to Amalthea. Thus Thebe's extra loss mechanism explains the differences in the size distributions observed by Galileo.

We find that the shadow resonance at Jupiter can simultaneously account for (1) the outward extension of the Thebe ring at constant inclination, (2) the gap interior to Thebe, (3) the large number of high-inclination particles, and (4) the excess of 0.2–0.3 μm grains at Amalthea in a natural model with only a single tunable parameter: the plasma density, which we constrain to $0.5\,cm^{-3} < n_e < 2.0\,cm^{-3}$. Changing other parameters of the plasma model will have similar effects to adjusting n_e, as ring particle dynamics is almost entirely determined by the details of the charging history (Fig. 3a). Shadow resonances are active to some extent in all diffuse dusty rings, and the vertical shadow resonance is a very promising mechanism for driving micrometre-sized ring particles to large latitudes. The origin of particles detected by the Voyager spacecraft at latitudes up to 30° near Saturn[17,18] remains an unsolved problem; we suggest that the vertical shadow resonance is a plausible solution.

Received 16 August 2007; accepted 28 February 2008.

1. Burns, J. A. *et al.* The formation of Jupiter's faint rings. *Science* **284,** 1146–1150 (1999).
2. Burns, J. A. *et al.* in *Jupiter: Planet, Satellites & Magnetosphere* (eds Bagenal, F., McKinnon, B. & Dowling, T.) 241–262 (Cambridge Univ. Press, Cambridge, UK, 2003).
3. Ockert-Bell, M. E. *et al.* The structure of Jupiter's ring system as revealed by the Galileo imaging experiment. *Icarus* **138,** 188–213 (1999).
4. Krüger, H. *Jupiter's Dust Disc, an Astrophysical Laboratory.* Thesis, Ruprecht-Karls-Universität (Shaker, Aachen, 2003).
5. Showalter, M. R., de Pater, I., Verbanac, G., Hamilton, D. P. & Burns, J. A. Properties and dynamics of Jupiter's gossamer rings from Galileo, Voyager, Hubble and Keck images. *Icarus*. (in the press).
6. Horányi, M. & Burns, J. A. Charged dust dynamics — Orbital resonance due to planetary shadows. *J. Geophys. Res.* **96,** 19283–19289 (1991).
7. de Pater, I. *et al.* Keck infrared observations of Jupiter's ring system near Earth's 1997 ring plane crossing. *Icarus* **138,** 214–223 (1999).
8. Throop, H. B. *et al.* The jovian rings: New results derived from Cassini, Galileo, Voyager and Earth-based observations. *Icarus* **172,** 59–77 (2004).
9. Showalter, M. R. *et al.* A new look at Jupiter's ring system: Preliminary results from New Horizons. *AAS/Div. Dyn. Astron. Meet.* 38, no. 12.07 (2007).
10. Grün, E. *et al.* The Galileo dust detector. *Space Sci. Rev.* **60,** 317–340 (1992).
11. Moissl, R. *Galileo's Staubmessungen in Jupiters Gossamer-Ringen.* Thesis, Ruprecht-Karls-Universität (2005).
12. Hamilton, D. P. & Burns, J. A. Ejection of dust from Jupiter's gossamer ring. *Nature* **364,** 695–699 (1993).
13. Schaffer, L. & Burns, J. A. Stochastic charging of dust grains in planetary rings: Diffusion rates and their effects on Lorentz resonances. *J. Geophys. Res.* **100,** 213–234 (1995).
14. Hamilton, D. P. Motion of dust in a planetary magnetosphere: Orbit-averaged equations for oblateness, electromagnetic, and radiation forces with application to Saturn's E ring. *Icarus* **101,** 244–264 (1993).
15. Hamilton, D. P. The asymmetric time-variable rings of Mars. *Icarus* **119,** 153–172 (1996).
16. Horányi, M., Morfill, G. E. & Grün, E. Mechanism for the acceleration and ejection of dust grains from Jupiter's magnetosphere. *Nature* **363,** 144–146 (1993).
17. Gurnett, D. A., Grün, E., Gallagher, D., Kurth, W. S. & Scarf, F. L. Micron-sized particles detected near Saturn by the Voyager plasma wave instrument. *Icarus* **53,** 236–254 (1983).
18. Srama, R. *et al.* In situ dust measurements in the inner Saturnian system. *Planet. Space Sci.* **54,** 967–987 (2006).
19. Horányi, M. & Cravens, T. E. The structure and dynamics of Jupiter's ring. *Nature* **381,** 293–298 (1996).

Acknowledgements We thank the Galileo project for a successful mission. This research was supported by grants from NASA Exobiology (D.P.H.) and DLR (H.K.).

Author Contributions H.K. did all of the data analysis and created Figs 1 and 2. D.P.H. did the analytic work and numerical modelling, including Figs 3 and 4.

Author Information Reprints and permissions information is available at www.nature.com/reprints. Correspondence and requests for materials should be addressed to D.P.H. (dphamil@umd.edu).